Validating Protection Settings of a Pipe-Type Cable Via Protective Relay Hardware-In-the-Loop Simulation

Zheyuan Cheng¹, Juergen Holbach¹, Munim Gani¹, and Benny Varughese²

¹Quanta Technology, Raleigh, NC, USA ²Consolidated Edison, New York, NY, USA

1 Abstract

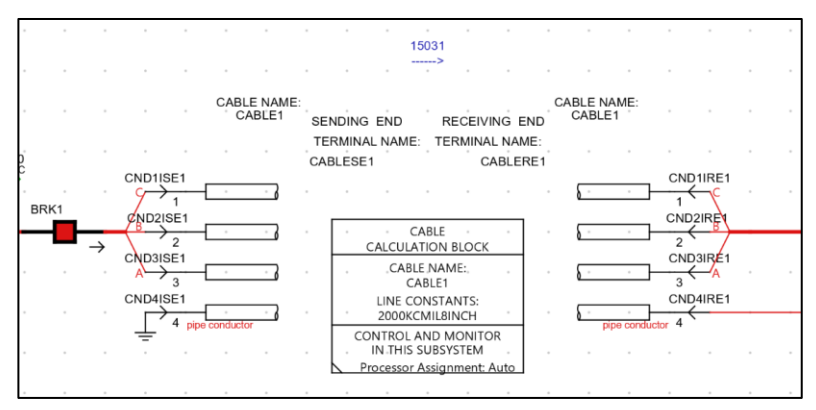
Underground high-pressure fluid-filled (HPFF) pipe-type cables are widely used for high-voltage transmission networks in densely populated urban areas. The protection setting development of these HPFF pipe-type cables is challenging, particularly because of its non-linear zero-sequence impedance. The zero-sequence impedance is dependent on the permeability of the steel pipe, which, in turn, is dependent on the zero-sequence current. As a result, the zero-sequence impedance becomes a non-linear function of fault current. There are, in general, two methods to calculate the zero-sequence impedance of an HPFF pipe-type cable: (1) empirical formula published by J. H. Neher in a 1960 paper, and (2) finite-element method considering detailed electromechanical dynamics. It is worth noting that currently, many commonly used short circuit programs (ASPEN and CAPE) and electromechanical transient (EMT) simulation programs (PSCAD and Simulink) do not support simulating this non-linear current-dependence effect out of the box.

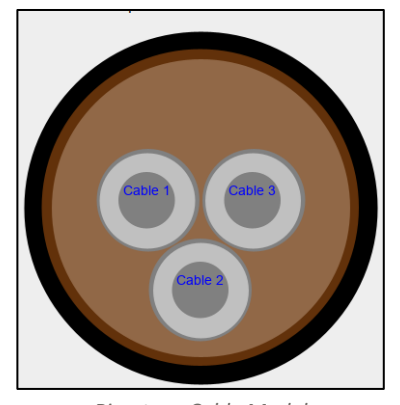
This paper introduces a novel method to accurately model the current-dependent HPFF pipe-type zero-sequence impedance in the Real-Time Digital Simulator (RTDS). This method not only accounts for current-dependent zero-sequence impedance, pipe cross-bounding, and system grounding but also enables hardware-in-the-loop simulation with protective relays to validate developed protection settings.

2 Pipe-Type Cable Modeling in RTDS

2.1 Limitation of the Pipe-Type Cable Model in RTDS

RTDS/RSCAD software provides a native pipe-type cable model (see Figure 1). It allows users to model pipe-type cable based on physical dimensions. Authors modeled two types of pipe-type cables—1500 KCMIL and 2000 KCMIL—based on cable specifications and drawings provided by Con Edison. However, we quickly learned that the simulated cable impedance is one order of magnitude different from the measured/calculated cable impedance value used in Con Edison's ASPEN and CAPE short circuit models. In addition to the impedance inaccuracy, we also learned that this model could not represent the non-linear zero-sequence impedance behavior well-known for pipe-type cables. Therefore, authors pivoted to other pipe-type cable modeling methods.





Model Snapshot in RSCAD

Pipe-type Cable Model

Figure 1. Native Pipe-Type Cable Model in RTDS/RSCAD

2.2 State-of-the-Art Pipe-Type Cable Modeling Methods and the Proposed Modeling Method

Authors conducted a literature review of pipe-type cable modeling and found two common approaches: 1) empirical formula methods and 2) finite-element methods. The most recognized method is an empirical formula method proposed by J. H. Neher [1]. This empirical formula method is computationally simple but has moderate accuracy, with a 19% error for R0 and a 35% error for X0. We could not use this method due to the technical barrier caused by the absence of many required measurement parameters. These parameters include conductor DC resistance, conductor loss factor, cable shield resistance, skid wire resistance, and others. For the finite element method, it provides significantly greater accuracy compared to empirical formula methods, but it necessitates extensive modeling efforts and is computationally intensive [2]. As this project requires the model to be simulated in real time, we consider this method too costly to run in RTDS.

Given the limitations of state-of-the-art methods, authors developed an novel modeling method for this project. This method assumes known non-linear zero-sequence impedance characteristics. For example, Figure 2 presents an example of non-linear zero-sequence impedance characteristics obtained from a cable manufacturer [3]. However, at the time of this project, such characteristics for the cables under test are not available. To proceed with the project, we assumed that Con Edison's cables follow similar characteristics. Based on our experience, we believe that this is a representative curve that can be used to approximate the cable in this project. According to Con Edison's measured/calculated cable data, the zero-sequence impedance is 2.04 Ohm @ 62.24 degrees with a 40 kA fault current. We have shifted the curves in Figure 2 to match this data point.

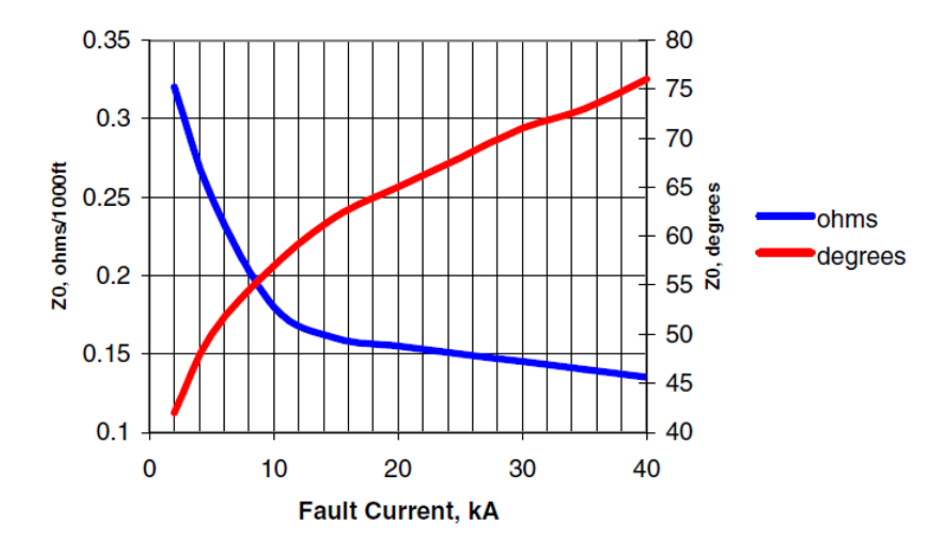


Figure 2. Example Non-Linear Zero-Sequence Impedance Characteristics [3]

Using the non-linear characteristics above, we can computationally determine the cable impedance for any fault location, type, and inception angle. Figure 3 depicts the proposed computation method for determining the cable impedance. The ASPEN model is first used to determine the zero-sequence impedance iteratively. For example, a fault is simulated with zero-sequence impedance at 40 kA. The resultant RMS phase current may be lower than 40 kA, and therefore, we need to look up the correct zero-sequence impedance from Figure 2 and repeat the fault simulation. We will eventually converge to a correct zero-sequence impedance value by performing this process iteratively. Once the zero-sequence impedance is determined, we will update the R and X values in the RTDS model shown in Figure 4 and perform a real-time HIL simulation with a protection relay. Note: This computational method will be used for each test scenario, as the fault current will vary at different fault locations or configurations.

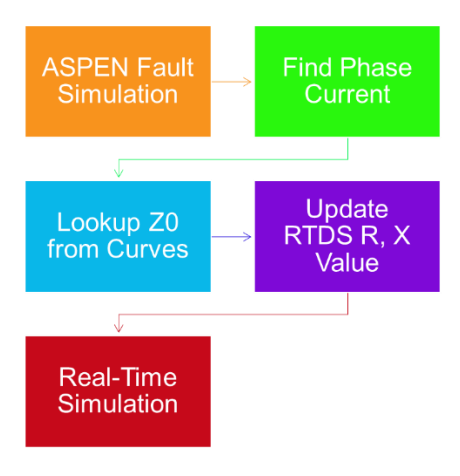


Figure 3. A Computational Method for Pipe-Type Cable Impedance Modeling

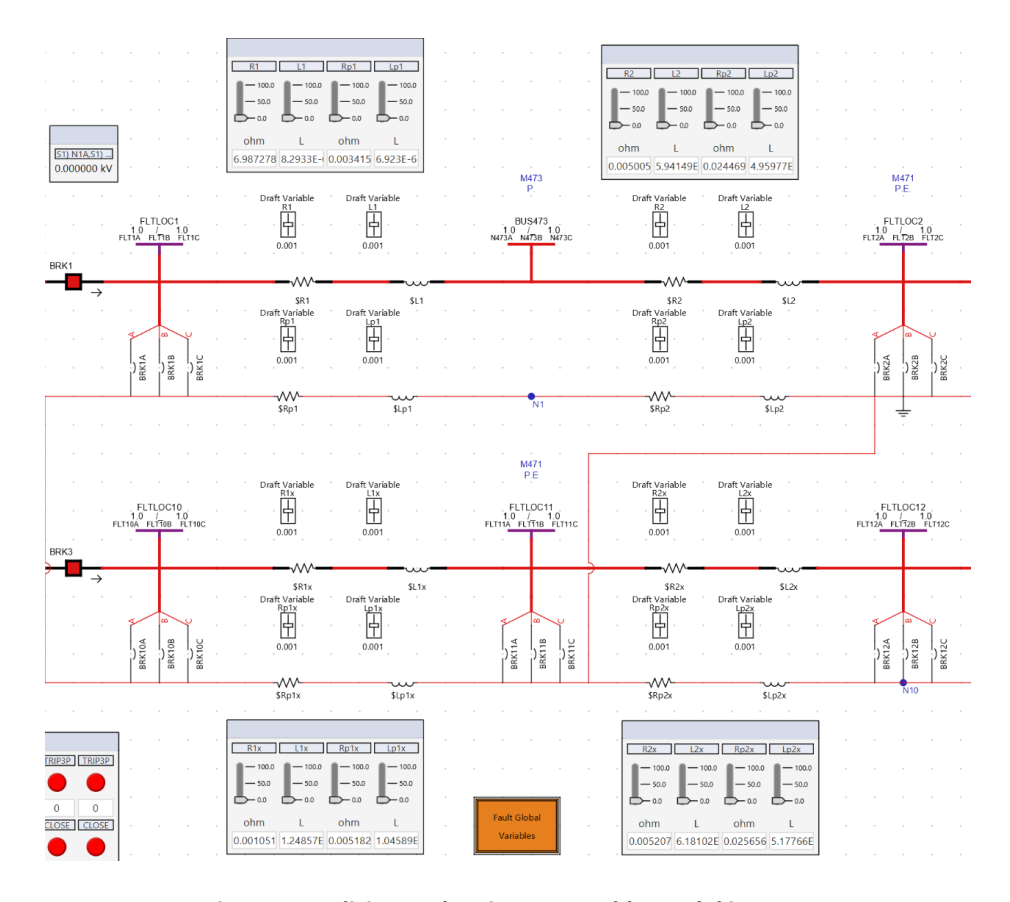


Figure 4. Explicit R and X Pipe Type Cable Model in RTDS

2.3 CT Saturation Modeling

Based on ASPEN studies, we observed that the fault current on one of the parallel cable can reach as high as 40 kA. Therefore, we believe it is necessary to model the CT saturation. At the time of this project, the exact CT models used in the substation were unclear to us. We assumed a C400 CT with a 2000/5 ratio for all four CTs (two CTs per terminal). Figure 5 presents the CT excitation curve we modeled in the RTDS [4].

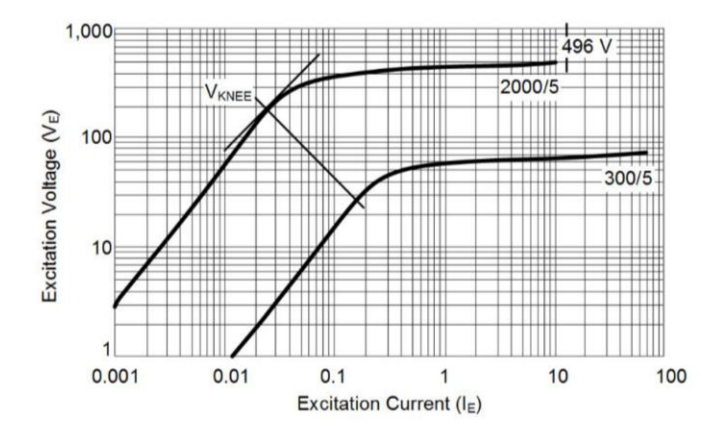


Figure 5. Example Excitation Graph for a C400 CT [4]

3 RTDS Testing Setup

The protective relays, i.e., SEL-411L and ABB RED670, and fiber communication are fully wired and commissioned in Quanta Technology's Raleigh RTDS lab (see Figure 6). The teleprotection circuit is configured based on the diagram in Figure 7. Note: The T1 carrier networks are represented using direct crossover Ethernet connections between the T1 switches.

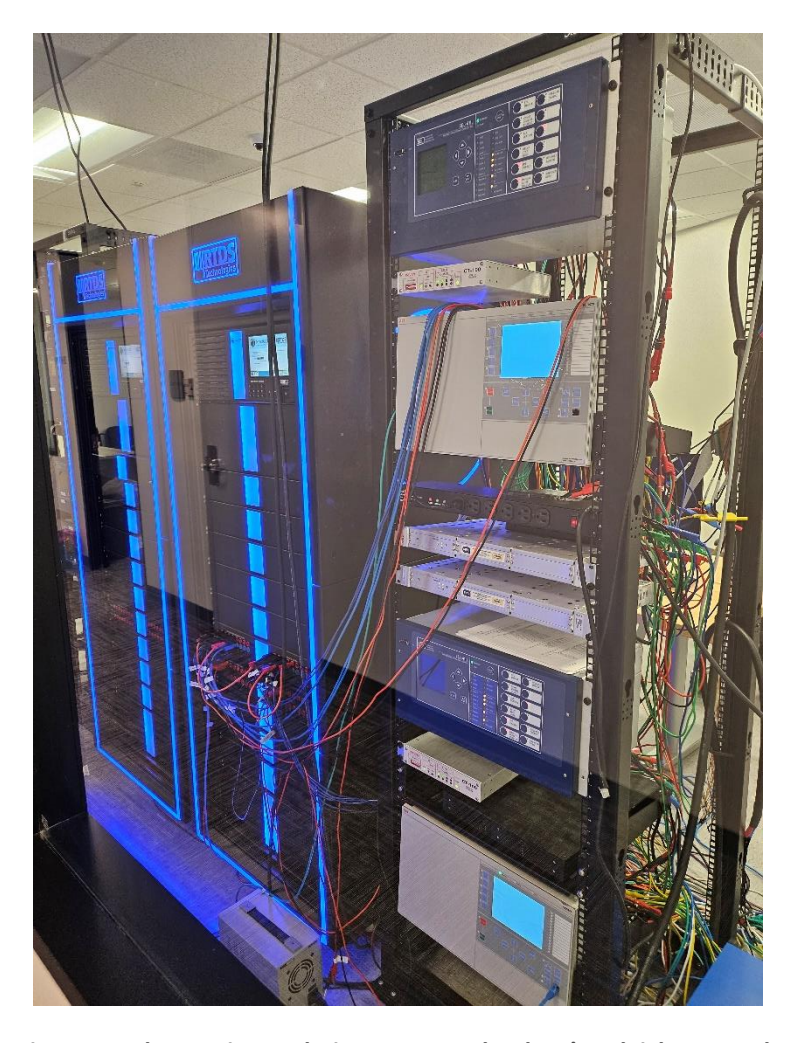


Figure 6. Relay Testing Racks in Quanta Technology's Raleigh RTDS Lab

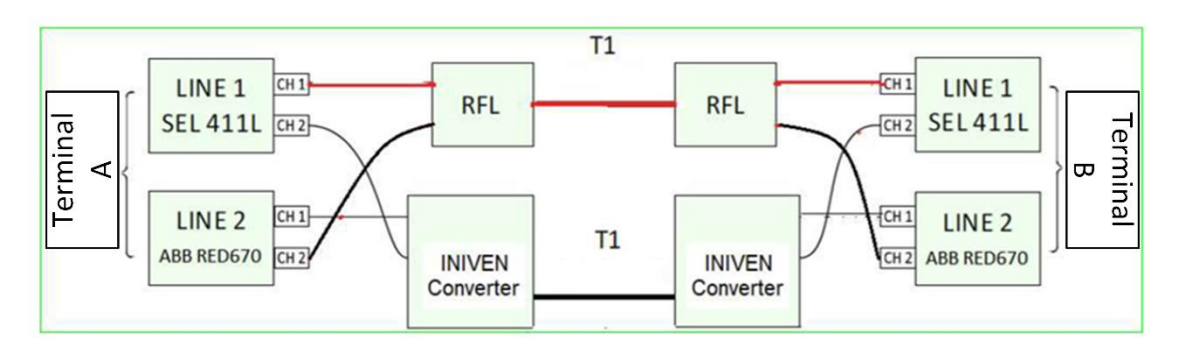


Figure 7. Teleprotection Circuits Used in the RTDS Test Setup

4 Test Plan for Protection Study

4.1 Reduced System Model

Based on the base ASPEN model, the reduced system model shown in Figure 8 is created in the RSCAD to represent the pipe-type cables and the surrounding system. Note: The underground cables going toward generator A and B are modeled for external fault simulation. Two equivalent boundaries approximate the rest of the system.

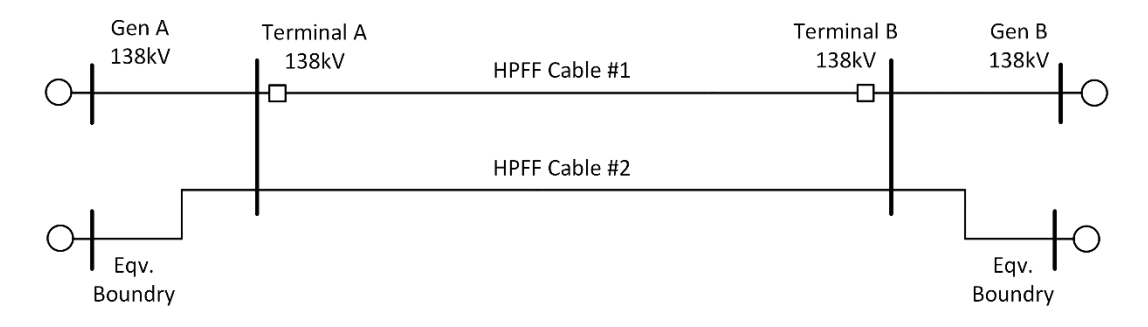


Figure 8. Reduced System One-line Diagram

4.2 Fault Locations

We designed a comprehensive set of internal and external faults to evaluate the protection performance. Figure 9 depicts nine fault locations within the first HPFF pipe-type cable. Similar fault locations will also be applied to the parallel pipe-type cable as external faults (labeled as P1 through P9). Figure 10 depicts two more external fault locations at 10% of the underground cables going toward the generators.

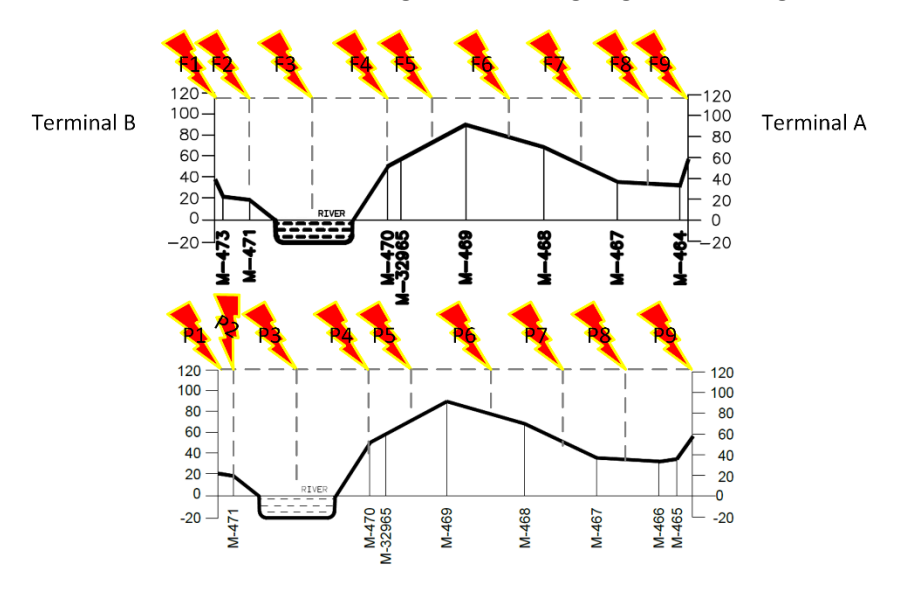


Figure 9. Internal Fault Locations

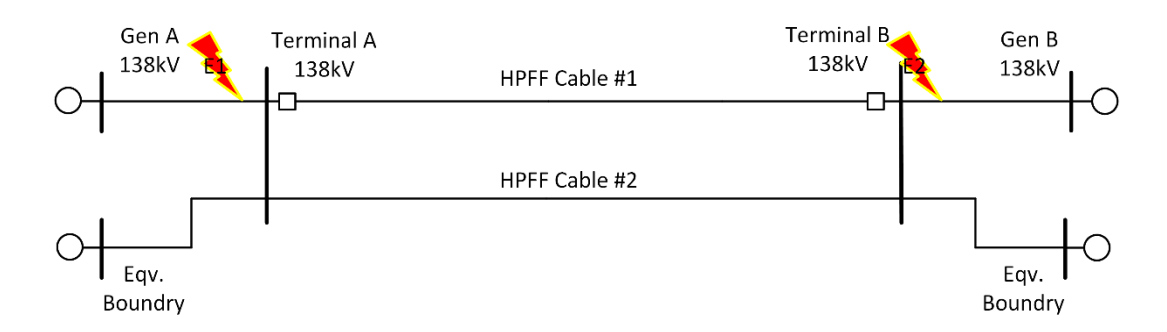


Figure 10. External Fault Locations

4.3 Fault Simulation

Figure 11 shows the fault simulation mechanism designed in this study. Due to the unique construction of pipe-type cable, we assume that all faults would involve the pipe conductor. Since the pipe conductor is grounded at two terminals and a few utility holes along the feeder, all faults are essentially ground faults. We will simulate three types of faults for this study: 1) AG, 2) BCG, and 3) ABCG faults. In addition to fault type configuration, we will simulate the fault at two different inception angles, i.e., 0-degree and 90-degree.

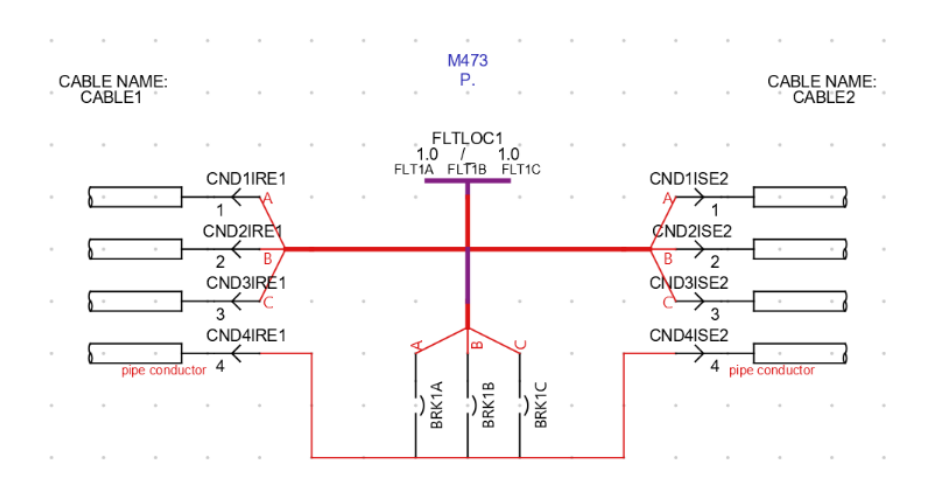


Figure 11. Pipe Type Cable Fault Simulation

4.4 Contingencies

To cover real-world contingencies, we considered the following two scenarios:

- Loss of 87 function (communication failure).
- 2. Loss of parallel line (HPFF pipe-type cable #2).

5 Test Results

5.1 Test with Normal System Conditions

In this test, we simulated faults with normal system conditions: 87 function active and parallel lines in service. Table 1 documents the test results for all internal faults under normal system conditions. The "TRIP_E_SEL" and "TRIP_E_ABB" signify the trip signal from the Terminal A SEL 411L relay and ABB RED670 relay, respectively. "TRIP_S_XXX" signifies the relays from the Terminal B side. The description "PU@0.0157"

means RTDS picks up the relay trip signal at 0.0157 sec after fault inception. Based on the results in Table 1, we can conclude that the 87 functions from both SEL411L and RED670 relays performed correctly.

Table 1. Internal Faults - Normal System Conditions

FLT_LOC T	FLT_TYP ▼	TRIP_E_SEL ~	TRIP_E_ABB ~	TRIP_S_SEL ~	TRIP_S_ABB ~
F1	ABCG	PU@0.0157;	PU@0.0262;	PU@0.0154;	PU@0.0202;
F1	AG	PU@0.0150;	PU@0.0216;	PU@0.0157;	PU@0.0238;
F1	BCG	PU@0.0154;	PU@0.0235;	PU@0.0155;	PU@0.0258;
F2	ABCG	PU@0.0146;	PU@0.0266;	PU@0.0154;	PU@0.0205;
F2	AG	PU@0.0163;	PU@0.0236;	PU@0.0167;	PU@0.0255;
F2	BCG	PU@0.0168;	PU@0.0266;	PU@0.0170;	PU@0.0208;
F3	ABCG	PU@0.0165;	PU@0.0249;	PU@0.0144;	PU@0.0271;
F3	AG	PU@0.0158;	PU@0.0247;	PU@0.0161;	PU@0.0270;
F3	BCG	PU@0.0156;	PU@0.0235;	PU@0.0159;	PU@0.0235;
F4	ABCG	PU@0.0167;	PU@0.0204;	PU@0.0163;	PU@0.0220;
F4	AG	PU@0.0160;	PU@0.0202;	PU@0.0150;	PU@0.0223;
F4	BCG	PU@0.0165;	PU@0.0221;	PU@0.0152;	PU@0.0242;
F5	ABCG	PU@0.0153;	PU@0.0226;	PU@0.0160;	PU@0.0219;
F5	AG	PU@0.0158;	PU@0.0270;	PU@0.0165;	PU@0.0212;
F5	BCG	PU@0.0163;	PU@0.0204;	PU@0.0151;	PU@0.0224;
F6	ABCG	PU@0.0163;	PU@0.0226;	PU@0.0168;	PU@0.0253;
F6	AG	PU@0.0166;	PU@0.0209;	PU@0.0149;	PU@0.0230;
F6	BCG	PU@0.0163;	PU@0.0242;	PU@0.0167;	PU@0.0270;
F7	ABCG	PU@0.0162;	PU@0.0219;	PU@0.0166;	PU@0.0240;
F7	AG	PU@0.0150;	PU@0.0268;	PU@0.0153;	PU@0.0209;
F7	BCG	PU@0.0160;	PU@0.0261;	PU@0.0161;	PU@0.0196;
F8	ABCG	PU@0.0153;	PU@0.0200;	PU@0.0156;	PU@0.0226;
F8	AG	PU@0.0149;	PU@0.0227;	PU@0.0158;	PU@0.0247;
F8	BCG	PU@0.0152;	PU@0.0235;	PU@0.0154;	PU@0.0259;
F9	ABCG	PU@0.0168;	PU@0.0217;	PU@0.0148;	PU@0.0237;
F9	AG	PU@0.0155;	PU@0.0232;	PU@0.0157;	PU@0.0255;
F9	BCG	PU@0.0155;	PU@0.0240;	PU@0.0155;	PU@0.0242;

Table 2 presents the test results for faults on the parallel line under normal system conditions. We can observe that the distance relays on the Terminal B have a longer reach than the Terminal A. Relays on both terminals operated on faults within their respective zone 2 reach with a 0.5-second delay. Note: The P4 fault location is right on the boundary of zone 2. Therefore, the relays did not operate on all faults at P4. Overall, the distance protection operated correctly and as expected for the faults on the parallel line.

Table 2. Faults on Parallel Line - Normal System Conditions

FLT_LOC T	FLT_TYP *	TRIP_E_SEL ~	TRIP_E_ABB ▼	TRIP_S_SEL ~	TRIP_S_ABB ~
P1	ABCG	PU@0.5192;	PU@0.5272;	No Op.	No Op.
P1	AG	PU@0.5221;	PU@0.5315;	No Op.	No Op.
P1	BCG	PU@0.5194;	PU@0.5252;	No Op.	No Op.
P2	ABCG	PU@0.5183;	PU@0.5218;	No Op.	No Op.
P2	AG	PU@0.5230;	PU@0.5236;	No Op.	No Op.
P2	BCG	PU@0.5177;	PU@0.5205;	No Op.	No Op.
P3	ABCG	PU@0.5196;	PU@0.5296;	No Op.	No Op.
P3	AG	PU@0.5214;	PU@0.5290;	No Op.	No Op.
P3	BCG	PU@0.5196;	PU@0.5240;	No Op.	No Op.
P4	ABCG	No Op.	No Op.	No Op.	No Op.
P4	AG	PU@0.5228;	PU@0.5440;	No Op.	No Op.
P4	BCG	No Op.	PU@0.5427;	No Op.	No Op.
P5	ABCG	No Op.	No Op.	No Op.	No Op.
P5	AG	No Op.	No Op.	No Op.	No Op.
P5	BCG	No Op.	No Op.	No Op.	No Op.
P6	ABCG	No Op.	No Op.	No Op.	No Op.
P6	AG	No Op.	No Op.	No Op.	No Op.
P6	BCG	No Op.	No Op.	No Op.	No Op.
P7	ABCG	No Op.	No Op.	No Op.	No Op.
P7	AG	No Op.	No Op.	No Op.	No Op.
P7	BCG	No Op.	No Op.	No Op.	No Op.
P8	ABCG	No Op.	No Op.	No Op.	No Op.
P8	AG	No Op.	No Op.	No Op.	No Op.
P8	BCG	No Op.	No Op.	No Op.	No Op.
P9	ABCG	No Op.	No Op.	PU@0.5193;	PU@0.5197;
P9	AG	No Op.	No Op.	PU@0.5228;	PU@0.5326;
P9	BCG	No Op.	No Op.	PU@0.5197;	PU@0.5216;

Table 3 presents the test results for external faults behind the line terminals. As these fault locations are beyond zone 2's reach, relays from both terminals are restrained from any operation. All relays performed correctly in this test.

Table 3. External Faults Behind the Terminal – Normal System Conditions

FLT_LOC •	FLT_TYP ~	TRIP_E_SEL *	TRIP_E_ABB *	TRIP_S_SEL ~	TRIP_S_ABB ~
E1	ABCG	No Op.	No Op.	No Op.	No Op.
E1	AG	No Op.	No Op.	No Op.	No Op.
E1	BCG	No Op.	No Op.	No Op.	No Op.
E2	ABCG	No Op.	No Op.	No Op.	No Op.
E2	AG	No Op.	No Op.	No Op.	No Op.
E2	BCG	No Op.	No Op.	No Op.	No Op.

5.2 Test Without 87 Function

Table 4 presents the internal fault test cases without 87 function. Zone 1's operations are color-coded in green, whereas zone 2's are color-coded in blue. Note: The fault location F5 is right at the boundary of zone 1's reach of the Terminal A relays. Therefore, we observed mixed zone 1 and 2 operations. Overall, the distance relay performed correctly and as expected.

Table 4. Internal Faults – Without 87 Function

FLT_LOC •	FLT_TYP •	TRIP_E_SEL *	TRIP_E_ABB ~	TRIP_S_SEL ~	TRIP_S_ABB 🕶
F1	ABCG	PU@0.5188;	PU@0.5240;	PU@0.0256;	PU@0.0209;
F1	AG	PU@0.5207;	PU@0.5244;	PU@0.0259;	PU@0.0209;
F1	BCG	PU@0.5194;	PU@0.5210;	PU@0.0267;	PU@0.0225;
F2	ABCG	PU@0.5183;	PU@0.5258;	PU@0.0253;	PU@0.0196;
F2	AG	PU@0.5203;	PU@0.5247;	PU@0.0252;	PU@0.0218;
F2	BCG	PU@0.5196;	PU@0.5218;	PU@0.0263;	PU@0.0182;
F3	ABCG	PU@0.5192;	PU@0.5242;	PU@0.0239;	PU@0.0212;
F3	AG	PU@0.5213;	PU@0.5233;	PU@0.0259;	PU@0.0216;
F3	BCG	PU@0.5173;	PU@0.5238;	PU@0.0267;	PU@0.0208;
F4	ABCG	PU@0.5182;	PU@0.5218;	PU@0.0255;	PU@0.0203;
F4	AG	PU@0.5205;	PU@0.5205;	PU@0.0253;	PU@0.0204;
F4	BCG	PU@0.5192;	PU@0.5243;	PU@0.0266;	PU@0.0210;
F5	ABCG	PU@0.5167;	PU@0.5236;	PU@0.0278;	PU@0.0209;
F5	AG	PU@0.0350;	PU@0.0398;	PU@0.0272;	PU@0.0194;
F5	BCG	PU@0.5180;	PU@0.0420;	PU@0.0270;	PU@0.0188;
F6	ABCG	PU@0.0264;	PU@0.0232;	PU@0.0269;	PU@0.0379;
F6	AG	PU@0.0285;	PU@0.0229;	PU@0.0353;	PU@0.0197;
F6	BCG	PU@0.0275;	PU@0.0215;	PU@0.0278;	PU@0.0217;
F7	ABCG	PU@0.0252;	PU@0.0222;	PU@0.5160;	PU@0.5246;
F7	AG	PU@0.0272;	PU@0.0235;	PU@0.5200;	PU@0.5225;
F7	BCG	PU@0.0273;	PU@0.0205;	PU@0.5195;	PU@0.5260;
F8	ABCG	PU@0.0251;	PU@0.0218;	PU@0.5176;	PU@0.5223;
F8	AG	PU@0.0254;	PU@0.0230;	PU@0.5224;	PU@0.5246;
F8	BCG	PU@0.0260;	PU@0.0192;	PU@0.5180;	PU@0.5200;
F9	ABCG	PU@0.0244;	PU@0.0217;	PU@0.5188;	PU@0.5255;
F9	AG	PU@0.0244;	PU@0.0200;	PU@0.5212;	PU@0.5274;
F9	BCG	PU@0.0271;	PU@0.0240;	PU@0.5193;	PU@0.5213;

Table 5 presents the test results for faults on the parallel line without 87 function. As expected, the zone 2 distance relays operated correctly and exhibited the same behavior shown in Table 2.

Table 5. Faults on Parallel Line – Without 87 Function

FLT_LOC T	FLT_TYP ▼	TRIP_E_SEL ~	TRIP_E_ABB ~	TRIP_S_SEL *	TRIP_S_ABB ~
P1	ABCG	PU@0.5196;	PU@0.5247;	No Op.	No Op.
P1	AG	PU@0.5222;	PU@0.5205;	No Op.	No Op.
P1	BCG	PU@0.5193;	PU@0.5197;	No Op.	No Op.
P2	ABCG	PU@0.5193;	PU@0.5225;	No Op.	No Op.
P2	AG	PU@0.5220;	PU@0.5193;	No Op.	No Op.
P2	BCG	PU@0.5183;	PU@0.5246;	No Op.	No Op.
P3	ABCG	PU@0.5200;	PU@0.5319;	No Op.	No Op.
P3	AG	PU@0.5229;	PU@0.5350;	No Op.	No Op.
P3	BCG	PU@0.5196;	PU@0.5260;	No Op.	No Op.
P4	ABCG	No Op.	No Op.	No Op.	No Op.
P4	AG	PU@0.5241;	PU@0.5432;	No Op.	No Op.
P4	BCG	No Op.	PU@0.5407;	No Op.	No Op.
P5	ABCG	No Op.	No Op.	No Op.	No Op.
P5	AG	No Op.	No Op.	No Op.	No Op.
P5	BCG	No Op.	No Op.	No Op.	No Op.
P6	ABCG	No Op.	No Op.	No Op.	No Op.
P6	AG	No Op.	No Op.	No Op.	No Op.
P6	BCG	No Op.	No Op.	No Op.	No Op.
P7	ABCG	No Op.	No Op.	No Op.	No Op.
P7	AG	No Op.	No Op.	No Op.	No Op.
P7	BCG	No Op.	No Op.	No Op.	No Op.
P8	ABCG	No Op.	No Op.	No Op.	No Op.
P8	AG	No Op.	No Op.	No Op.	No Op.
P8	BCG	No Op.	No Op.	No Op.	No Op.
P9	ABCG	No Op.	No Op.	PU@0.5175;	PU@0.5225;
P9	AG	No Op.	No Op.	PU@0.5220;	PU@0.5331;
P9	BCG	No Op.	No Op.	PU@0.5182;	PU@0.5232;

Table 6 presents the test results for faults behind the terminal when the 87 function is lost. As expected, the relays were all restrained from operation and behaved correctly.

Table 6. External Faults Behind the Terminal – Without 87 Function

FLT_LOC •	FLT_TYP ~	TRIP_E_SEL ~	TRIP_E_ABB ▼	TRIP_S_SEL *	TRIP_S_ABB *
E1	ABCG	No Op.	No Op.	No Op.	No Op.
E1	AG	No Op.	No Op.	No Op.	No Op.
E1	BCG	No Op.	No Op.	No Op.	No Op.
E2	ABCG	No Op.	No Op.	No Op.	No Op.
E2	AG	No Op.	No Op.	No Op.	No Op.
E2	BCG	No Op.	No Op.	No Op.	No Op.

5.3 Test When the Parallel Line Is Out-of-Service

This section presents the test results when the parallel line is out of service. Table 7 shows that the 87 functions from all relays can clear all internal faults at high speed. Table 8 presents that all distance relays can restrain the operation for external faults beyond zone 2 reach. Both test cases showed the correct relay responses.

Table 7. Internal Faults - Parallel Line Out-of-Service

FLT_LOC •	FLT_TYP -	TRIP_E_SEL ▼	TRIP_E_ABB ~	TRIP_S_SEL ~	TRIP_S_ABB 🔻
F1	ABCG	PU@0.0144;	PU@0.0197;	PU@0.0139;	PU@0.0216;
F1	AG	PU@0.0157;	PU@0.0249;	PU@0.0149;	PU@0.0267;
F1	BCG	PU@0.0155;	PU@0.0225;	PU@0.0152;	PU@0.0242;
F2	ABCG	PU@0.0136;	PU@0.0268;	PU@0.0147;	PU@0.0206;
F2	AG	PU@0.0137;	PU@0.0262;	PU@0.0149;	PU@0.0204;
F2	BCG	PU@0.0149;	PU@0.0251;	PU@0.0149;	PU@0.0265;
F3	ABCG	PU@0.0155;	PU@0.0240;	PU@0.0136;	PU@0.0232;
F3	AG	PU@0.0147;	PU@0.0235;	PU@0.0146;	PU@0.0232;
F3	BCG	PU@0.0150;	PU@0.0256;	PU@0.0148;	PU@0.0195;
F4	ABCG	PU@0.0151;	PU@0.0232;	PU@0.0148;	PU@0.0244;
F4	AG	PU@0.0138;	PU@0.0257;	PU@0.0140;	PU@0.0192;
F4	BCG	PU@0.0159;	PU@0.0247;	PU@0.0160;	PU@0.0243;
F5	ABCG	PU@0.0152;	PU@0.0232;	PU@0.0156;	PU@0.0225;
F5	AG	PU@0.0143;	PU@0.0267;	PU@0.0140;	PU@0.0205;
F5	BCG	PU@0.0145;	PU@0.0278;	PU@0.0142;	PU@0.0219;
F6	ABCG	PU@0.0141;	PU@0.0232;	PU@0.0143;	PU@0.0251;
F6	AG	PU@0.0141;	PU@0.0211;	PU@0.0141;	PU@0.0227;
F6	BCG	PU@0.0140;	PU@0.0262;	PU@0.0136;	PU@0.0202;
F7	ABCG	PU@0.0138;	PU@0.0255;	PU@0.0138;	PU@0.0189;
F7	AG	PU@0.0135;	PU@0.0227;	PU@0.0142;	PU@0.0224;
F7	BCG	PU@0.0147;	PU@0.0281;	PU@0.0154;	PU@0.0219;
F8	ABCG	PU@0.0147;	PU@0.0236;	PU@0.0149;	PU@0.0207;
F8	AG	PU@0.0143;	PU@0.0235;	PU@0.0140;	PU@0.0233;
F8	BCG	PU@0.0155;	PU@0.0228;	PU@0.0155;	PU@0.0275;
F9	ABCG	PU@0.0137;	PU@0.0195;	PU@0.0142;	PU@0.0211;
F9	AG	PU@0.0152;	PU@0.0246;	PU@0.0148;	PU@0.0232;
F9	BCG	PU@0.0137;	PU@0.0246;	PU@0.0147;	PU@0.0206;

Table 8. External Faults Behind the Terminal – Parallel Line Out-of-Service

FLT_LOC T	FLT_TYP *	TRIP E SEL *	TRIP_E_ABB ~	TRIP S SEL *	TRIP_S_ABB ~
E1	ABCG	No Op.	No Op.	No Op.	No Op.
E1	AG	No Op.	No Op.	No Op.	No Op.
E1	BCG	No Op.	No Op.	No Op.	No Op.
E2	ABCG	No Op.	No Op.	No Op.	No Op.
E2	AG	No Op.	No Op.	No Op.	No Op.
E2	BCG	No Op.	No Op.	No Op.	No Op.

5.4 Test When the Parallel Line Is Out-of-Service, and There Is Loss of 87 Function

Table 9 presents the internal fault test cases without 87 function. Zone 1's operations are color-coded in green, whereas zone 2's are color-coded in blue. Note: The fault location F5 is right at the boundary of zone 1's reach of the Terminal A relays. Therefore, we observed mixed zone 1 and 2 operations. Overall, the distance relay performed correctly and as expected. Table 10 presents that all distance relays can restrain the operation for external faults beyond zone 2 reach. Both test cases showed the correct relay responses.

FLT LOC TFLT TYP TRIP E SEL TRIP E ABB TRIP S SEL TRIP S ABB ABCG PU@0.5172; PU@0.5224; PU@0.0250; F1 AG PU@0.5203; PU@0.5239; PU@0.0255; PU@0.0232; F1 PU@0.5894; PU@0.5244; BCG PU@0.0263; PU@0.0214; F2 ABCG PU@0.5165: PU@0.5244: PU@0.0238; PU@0.0225: F2 PU@0.5194; PU@0.5213; PU@0.0268; PU@0.0228: AG BCG PU@0.5915; PU@0.5239; PU@0.0261; PU@0.0237; F3 PU@0.5159; PU@0.5252; PU@0.0258; **ABCG** PU@0.0217; F3 AG PU@0.5200; PU@0.5192; PU@0.0274; PU@0.0209; F3 BCG PU@0.5871; PU@0.5237; PU@0.0262; PU@0.0202; PU@0.5160; PU@0.5189; F4 PU@0.0255; PU@0.0202; ABCG F4 PU@0.5204; PU@0.5195; PU@0.0275; PU@0.0210; AG F4 BCG PU@0.5188; PU@0.5220; PU@0.0267; PU@0.0198; F5 ABCG PU@0.5173; PU@0.5238; PU@0.0265; PU@0.0235; F5 PU@0.0365; PU@0.0278; PU@0.0295; AG PU@0.0240; F5 BCG PU@0.5188; PU@0.0187; PU@0.0261; PU@0.0203; F6 ABCG PU@0.0275; PU@0.0208; PU@0.0265; PU@0.0404; F6 PU@0.0288; PU@0.0200; PU@0.0365; PU@0.0320; AG F6 BCG PU@0.0270; PU@0.0206; PU@0.0283; PU@0.0220; F7 ABCG PU@0.0253; PU@0.0213; PU@0.5161; PU@0.5228; PU@0.0285; PU@0.0195; PU@0.5195; PU@0.5209; F7 AG F7 BCG PU@0.0269; PU@0.0200; PU@0.5174; PU@0.5242; F8 PU@0.0239; PU@0.0184; PU@0.5168; PU@0.5247; ABCG F8 AG PU@0.0267; PU@0.0210; PU@0.5212; PU@0.5231; F8 BCG PU@0.0260; PU@0.0225; PU@0.5900; PU@0.5262; F9 ABCG PU@0.0250; PU@0.0188; PU@0.5162; PU@0.5202; F9 AG PU@0.0273; PU@0.0220; PU@0.5198; PU@0.5233; F9 BCG PU@0.0256; PU@0.0210; PU@0.5980; PU@0.5244;

Table 9. Internal Faults - Parallel Line Out-of-Service and Loss of 87 Function

Table 10. External Faults Behind the Terminal - Parallel Line Out-of-Service and Loss of 87 Function

FLT_LOC 3	FLT_TYP ▼	TRIP_E_SEL ▼	TRIP_E_ABB ▼	TRIP_S_SEL ~	TRIP_S_ABB ▼
E1	ABCG	No Op.	No Op.	No Op.	No Op.
E1	AG	No Op.	No Op.	No Op.	No Op.
E1	BCG	No Op.	No Op.	No Op.	No Op.
E2	ABCG	No Op.	No Op.	No Op.	No Op.
E2	AG	No Op.	No Op.	No Op.	No Op.
E2	BCG	No Op.	No Op.	No Op.	No Op.

6 Conclusions

This paper introduces a novel method to accurately model the current-dependent HPFF pipe-type zero-sequence impedance in the RTDS. This method not only accounts for current-dependent zero-sequence impedance, pipe cross-bounding, and system grounding but also enables hardware-in-the-loop simulation with protective relays to validate developed protection settings. Authors designed a set of comprehensive test cases to evaluate the protection settings for a pipe-type cable in Con Edison's system. Authors were able to successfully validate the protection settings developed for two relay models (SEL411L and ABB RED670) via RTDS relay HIL testing.

7 References

- [1] J. H. Neher, "The phase sequence impedance of pipe-type cables", IEEE Trans. Power Apparat. Syst., vol. PAS-83, pp. 795-804, Aug. 1964. doi: 10.1109/TPAS.1964.4766076.
- [2] Xiao-Bang Xu, Guanghao Liu and P. Chow, "A finite-element method solution of the zero-sequence impedance of underground pipe-type cable," in IEEE Transactions on Power Delivery, vol. 17, no. 1, pp. 13-17, Jan. 2002. doi: 10.1109/61.974182.
- [3] B. Kasztenny, I. Voloh and J. G. Hubertus, "Applying distance protection to cable circuits," 57th Annual Conference for Protective Relay Engineers, 2004, College Station, TX, USA, 2004, pp. 46-69, doi: 10.1109/CPRE.2004.238353.
- [4] Ariana Hargrave, Michael J. Thompson, and Brad Heilman, "Beyond the Knee Point: A Practical Guide to CT Saturation," in 44th Annual Western Protective Relay Conference, October 2017. doi: 10.1109/CPRE.2018.8349779.

8 Author Biography

Zheyuan Cheng received his Ph.D. degree in Electrical Engineering from North Carolina State University in 2020 and his B.Eng. degree in electrical engineering from Nanjing University of Aeronautics and Astronautics in 2015. He has held various roles of increasing responsibility since he joined Quanta Technology in 2020. He holds one US patent and has published over twenty IEEE journal papers and conference proceedings. He is a recipient of the 2021 Best Paper Award from IEEE Industrial Electronics Magazine.

Juergen Holbach, PHD, EXECUTIVE ADVISOR, Senior Director of Automation and Testing, has over 30 years of experience designing and applying protective relaying. He has published over a dozen papers and holds three patents. Juergen is a Western Protective Relay Conference (WPRC) Planning Committee member. Juergen's areas of expertise include automation and protection, inverter-based resource (IBR) impact of protection, real-time digital simulator (RTDS) testing, and International Electrotechnical Commission (IEC) 61850 compliance.

Munim Bin Gani (Member, IEEE) received the B.Sc degree in Electrical Engineering (EE) from Bangladesh University of Engineering and Technology, Dhaka, Bangladesh in 2011, the M.Sc in EE from New Mexico State University, Las Cruces, New Mexico in 2018 and Ph.D. in EE from Clemson University, South Carolina in 2023. He is currently working as Principal Engineer at Quanta Technology LLC, Raleigh, North Carolina . His research interests include power system modeling and protection, DC/AC/Hybrid microgrids, dynamic simulation of power system.

Benny Varughese received his Bachelor of Science in Electrical Engineering from Drexel University and his Master of Science in Electrical Engineering from Manhattan College. He has over 20 years of experience in the electric utility industry. He has held positions of increasing responsibility in substation and engineering. He was a substation Equipment and Field Engineer supporting Substation Operations and a Protective Relay Testing Supervisor and Manager for Substations Operations. He has also worked as a Commissioning Engineer in Substations working with various utilities; he is currently a Senior Engineer for the Protective Relay Strategy and Implementation group.